Application of hybrid coagulation–ultrafiltration for decentralized drinking water treatment: impact on flux, water quality and costs

S. G. Arhin, N. Banadda, A. J. Komakech, W. Pronk and S. J. Marks

ABSTRACT

Decentralized membrane-based water treatment represents an attractive and viable approach to safe water supply in low-income areas, but its widespread adoption requires cost-effective antifouling strategies. Although the antifouling mechanisms of Al-based coagulants have been widely investigated, there is little data about their impact on costs and treatment efficiency for decentralized membrane-based systems. In this study, a comparative assessment of two decentralized ultrafiltration (UF) units with and without polyaluminum chloride (PACl) coagulation was undertaken to evaluate the influence of coagulation on the fouling, water quality, and costs nexus. The results showed that PACl suppressed both total fouling and hydraulically irreversible fouling. A matched-pair analysis also revealed that PACl improved the permeate quality by enhancing the removal of particulates and dissolved organics. Compared with the conventional UF system, the hybrid coagulation–UF system contributed to a 21% increase in the flux rate, allowing for a 27% reduction in membrane area and thus, providing cost benefits in terms of both capital and operating costs. These results suggest that PACl coagulation is potentially a cost-effective antifouling method for decentralized membrane-based water systems.

Key words | coagulation, costs, decentralized treatment, membrane fouling, ultrafiltration

S. G. Arhin (corresponding author)
N. Banadda
A. J. Komakech
Department of Agricultural and Biosystems Engineering,
Makerere University,
P.O. Box 7062, Kampala,
Uganda
E-mail: arhinsamuel32@gmail.com

S. G. Arhin
W. Pronk
S. J. Marks
Eawag: Swiss Federal Institute of Aquatic Science and Technology,
Überlandstrasse 133, 8600 Dübendorf,
Switzerland

N. Banadda
Department of Agricultural and Biosystems Engineering,
Iowa State University,
1340 Elings Hall, Ames, IA, 50011–32700,
USA

INTRODUCTION

Inadequate access to safe drinking water imperils life, subdues opportunity and subverts human dignity (Watkins 2006). Yet 2.1 billion people – 29% of the global population – lack safely managed drinking water services (WHO/ UNICEF 2017). Low-income countries (LIC) are disproportionately affected by the pernicious and persistent water crisis of today, underpinned by a shortage of fresh water resources due to climate change and escalating levels of water pollution. In many LIC, drinking water treatment is mainly focused on conventional technologies such as media filtration and chlorine disinfection. However, conventional technologies are designed for use in large centralized systems. Therefore, they are highly unlikely to be installed in rural communities due to their high investment costs.

Nowadays, decentralized membrane-based water treatment has emerged as a sustainable approach to safe water supply in LIC. However, membrane fouling remains an overriding obstacle. To alleviate fouling, raw water pretreatment using techniques such as coagulation, biofiltration, adsorption, and oxidation has been widely proposed. Among these techniques, coagulation remains the most successful method for controlling membrane fouling in full-scale water treatment (Arhin *et al.* 2016).

Aluminum sulfate is the most commonly used coagulant and can suppress the hydraulically irreversible fouling rate of hollow fiber membranes by 75–100% (Hatt *et al.* 2011). However, currently, there is an upsurge in the use of pre-hydrolyzed coagulants, including polyaluminum chloride (PACl). PACl contains substantial proportions of highly charged tridecamer cationic species (Al$_{13}$), which are effective in neutralizing negatively charged colloids (Arhin *et al.* 2018). Much work has been aimed at expounding the antifouling mechanisms of coagulants and at identifying coagulation conditions most effective for fouling abatement (Howe & Clark 2006). Promising results seem to be contingent on the coagulant type, dosage, mixing conditions, flow configuration, membrane properties, and feed water characteristics. Although a plethora of coagulation–ultrafiltration (UF) studies have reported favorable results with regards to contaminant elimination and flux amelioration, studies on the impact of coagulation on treatment costs are relatively rare. Yet, information in this regard is essential for the widespread adoption of such systems in LIC.

The aim of this study was, therefore, to evaluate the influence of coagulation on the performance of a pilot-scale UF unit for decentralized water treatment in terms of flux, water quality, and costs. Although the hybrid coagulation–UF system is rarely applied in LIC, we presume it could represent a potentially cost-effective approach to alleviating the drinking water crisis in LIC. This hypothesis is premised on the diminishing cost of UF membranes, the relatively low cost of coagulants and the need to deal with freshwater quality problems in LIC, including eutrophication, cyanobacteria, and disinfection by-product precursors, which make conventional treatments rather costly.

MATERIALS AND METHODS

Feed water and study area

The feed water used in this study was collected from Lake Victoria – at the inlet to Ggaba II Water Treatment Plant, Kampala, Uganda. The characteristics of the feed water (Table A1) and further information on the study area are presented in the Appendix (available with the online version of this paper).

Pilot-scale ultrafiltration experiments

Two sets of UF experiments were used to assess the influence of PACl on flux, permeate quality and costs. In the first, commercial liquid PACl solution (Zetafloc 553 L; Abby Laboratories, South Africa) was used to pretreat the feed water prior to UF (herein denoted as system A). Coagulation pretreatment was performed using the optimum conditions observed during bench-scale tests as described previously: PACl dose of 20 mg·L^{-1}, corresponding to 1.21 mg-Al·L^{-1} and a hydraulic retention time of 14 min (Arhin *et al.* 2018). The pH of the raw water was not adjusted during coagulation in order to mimic full-scale conditions at the local water treatment plant. The setup for system A, therefore, was comprised of coagulation/flocculation followed by UF without sedimentation. In the second set of experiments (system B), the feed water was treated by UF without PACl coagulation (0 mg·L^{-1} PACl). The setup for the two systems is schematically shown in Figure A2, Appendix (available online).

The treatment efficiency of the two systems was assessed based on the removal of turbidity, color, dissolved organic carbon (DOC), ultraviolet absorbance at 254 nm (UVA$_{254}$) and specific UVA$_{254}$ absorbance (SUVA). Therefore, periodic samples of feed water and permeate were taken and the removal efficiency of each parameter (solute rejection, *R*) was quantified as:

$$R(\%) = \left[1 - \left(\frac{C_\mathrm{p}}{C_\mathrm{f}} \right) \right] \times 100 \tag{1}$$

where C_p and C_f are the permeate and feed concentrations, respectively.

The UF membranes used in this study were polysulfone (PS) hollow-fiber membranes (Frontec Environmental Co., Ltd, China) operated in an inside-out mode. A membrane module had an effective area of 4.5 m^2, a molecular weight cut-off (MWCO) of 100 kDa, a fiber outer diameter of 1.6 mm, and an inner diameter of 1.0 mm. Each experiment was conducted with a membrane in pristine condition. Prior to each experiment, the new membrane

was soaked in clean water for 24 h and flushed copiously to remove any residual storage agent. The baseline membrane specific flux, J_o, was determined by 30 min filtration of clean water. Filtration experiments were conducted in the dead-end mode under a transmembrane pressure of 30 kPa. The filtration cycle in each system was set at 60 min, and back-washing was done after each cycle with permeate for 5 min (flux, 80 L·h^{-1}·m^{-2}). The permeate flux, $J = Q/A$, was calculated from the permeate flow rate, Q (L·h^{-1}), and the membrane area, A (m^2). The calculated flux was then adjusted to the equivalent flux at standard temperature (20 °C) using the expression $J_s = J(1.03)^{T_s - T}$, where J_s is the flux at standard temperature (L·h^{-1} m^{-1}), T_s is the standard temperature (°C) and T is the measured temperature (°C) (Crittenden *et al.* 2012). The ratio of the equivalent flux at standard temperature, J_s, to the flux of clean water at standard temperature, J_{os}, was designated as the normalized specific flux, J_s/J_{os}, and was used for comparing the effect of each experiment. Chemical cleaning was done at the end of each experiment. The membranes were soaked in NaOCl (100 mg/L) for 3 h, followed by NaOH (0.02 N) for 3 h, then rinsed thoroughly with permeate.

Fouling rate quantification

The universal membrane fouling index (UMFI) was used to quantify the fouling rate in each system. The UMFI is defined as:

$$UMFI = \frac{J_s' - 1}{V_s} \tag{2}$$

where J_s' is the inverse of the normalized specific flux, J_s/J_{os} (dimensionless), with J_s being the specific flux (J/P), where J is the flux (m/s) and P the transmembrane pressure (Pa), and where J_{os} is the flux at time 0, and V_s is the unit permeate throughput (Lm^{-2}) (Huang *et al.* 2012). The UMFI for total fouling (UMFI$_T$) was determined by linear fitting of the experimental values of J_s' against V_s for each system (Figure A3, Appendix, available online). In comparison, the UMFI for hydraulically irreversible fouling (UMFI$_{IR}$) and the UMFI for chemically irreversible fouling (UMFI$_C$) were determined by inserting J_s' and V_s values obtained at the onset of hydraulic backwash and chemical cleaning, respectively, into Equation (2).

Analytical methods

DOC was measured by a TOC analyzer (Shimadzu TOC-VCPH, Japan). UVA$_{254}$ was quantified by UV spectrometry at 254 nm (photoLab 6600 UV-VIS, Germany). Samples for UVA$_{254}$ and DOC were pre-filtered with a 0.45 μm sterile membrane (MCNE–447–100; Labbox, France). Turbidity measurements were done with a portable turbidimeter (Hach 2100Q, USA). Color was quantified by UV spectrometry at 455 nm (Hach DR1900, USA). Conductivity and pH were measured with a Hach Sension+ multi-parameter meter (Hach MM374, USA). SUVA was determined from the ratio of UVA$_{254}$ and DOC as:

$$SUVA = 100 \times \left(\frac{UVA_{254}}{DOC} \right) \tag{3}$$

The microbiological quality of the permeate was assessed by using the Colilert-18 test kit based on the Most Probable Number method (American Public Health Association 2004). The log reduction value (LRV) was calculated as:

$$LRV = \log\left(\frac{C_f}{C_p} \right) \tag{4}$$

where C_f and C_p are the concentration of coliform bacteria in the feed water and permeate, respectively. When no coliform bacteria were detected in the permeate ($C_p < 1$ CFU/ 100 mL), LRV was reported as $>\log C_f$.

RESULTS AND DISCUSSION

Effect of polyaluminum chloride on permeate flux

The variations in the average normalized flux and UVA$_{254}$ removal rates for systems A and B are shown in Figure 1(a) and 1(b), respectively. As depicted in Figure 1(a), a two-stage flux decline mode consisting of a rapid flux decline during the initial filtration periods followed by a slow drop was observed in both systems, however, to varying extents. For system B the flux dropped rapidly to 58% on the 9th day.
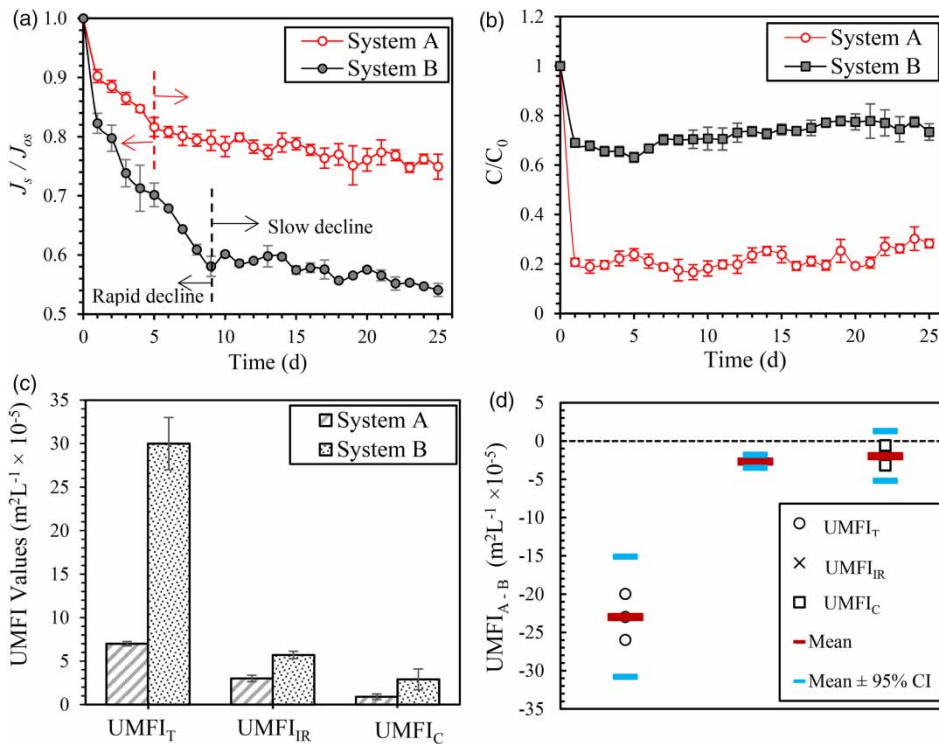
Figure 1 | (a) Changes in the normalized specific permeate flux for systems A and B. Daily flux data represents the mean of four filtration cycles with intermittent permeate backwash every 60 min (backwashing flux: 80 L m^{-2} h^{-1}, 5 min). (b) UVA$_{254}$ removal rate ($n = 3$), (c) UMFI values, and (d) matched-pair analysis for total, hydraulically irreversible, and chemically irreversible fouling in systems A and B ($n = 3$). The ordinate in (d) is expressed in terms of system A minus system B values.

This rapid flux decline was followed by a gradual decrease over the next duration of the experiment. In contrast, the flux for system A declined rapidly to 82% on the 5th day and this was followed by a relatively stabilized flux in the subsequent days.

This two-stage flux decline mode exhibited by the normalized flux curves suggests potential changes in the fouling mechanisms, as per the pore blockage–cake filtration model described in previous studies (Ho & Zydney 2000). The rapid flux decline observed during the initial filtration periods suggests that pore blocking was the most dominant fouling mechanism at that stage, attributable to the adsorption of UVA$_{254}$ on/in the membrane via hydrophobic interaction. However, this was followed by cake layer formation in the subsequent days. After 25 days of operation, the flux of system A was 21% higher than system B, suggesting that PACl coagulation could ameliorate permeate flux.

Figure 1(c) presents the nature and extent of fouling in systems A and B. A higher UMFI$_T$ value was observed in system B than in system A, suggesting that PACl was effective in reducing the total fouling rate. Furthermore, the value for UMFI$_{IR}$ that

indicates the residual fouling after hydraulic backwash was higher in system B than in system A, suggesting that hydraulically irreversible fouling was also suppressed by PACl coagulation. However, our results showed no distinction in the chemically irreversible fouling rate for the two systems. As shown by the matched-pair analysis in Figure 1(d), the line corresponding to $y = 0$ that shows whether the UMFI values for systems A and B are equal is within the mean ± 95% confidence interval (CI) range for UMFI$_C$, indicating that there was no statistical difference. This is probably due to the low levels of the UMFI$_C$ values in both systems (<0.00005 m^2 L^{-1}), which were difficult to quantify as previously observed (Huang *et al.* 2012).

Water quality

The quality of permeate produced from systems A and B in comparison with the local drinking water standards is presented in Table A3 (Appendix, available with the online version of this paper). As expected, UF was found to be very effective in removing pathogenic indicators (*E. coli*

and total coliforms), with zero indicator bacteria detectable in the permeate in both systems. However, besides bacteria removals, PACl coagulation enhanced the removal of all other aquatic contaminants monitored.

Turbidity and color were two key quality parameters monitored. From an operational perspective, these two parameters are usually indicative of the performance of the treatment processes and their ability to conform to appropriate water quality standards (Ho *et al.* 2012). Consistent with the results of previous coagulation–UF studies (Bergamasco *et al.* 2011), the

hybrid PACl-UF system was very effective in removing compounds responsible for turbidity and color. As shown in Figure 2(a), higher turbidity (99.2%) and color (100%) removal rates were attained in system A compared with system B (98.1% and 97.5%, respectively).

Besides turbidity and color, DOC removal also increased with PACl coagulation. However, DOC is only a measure of the dissolved NOM concentration and does not reflect the characteristics of the NOM. Thus, in a further step, the degree of conjugation and aromaticity in the
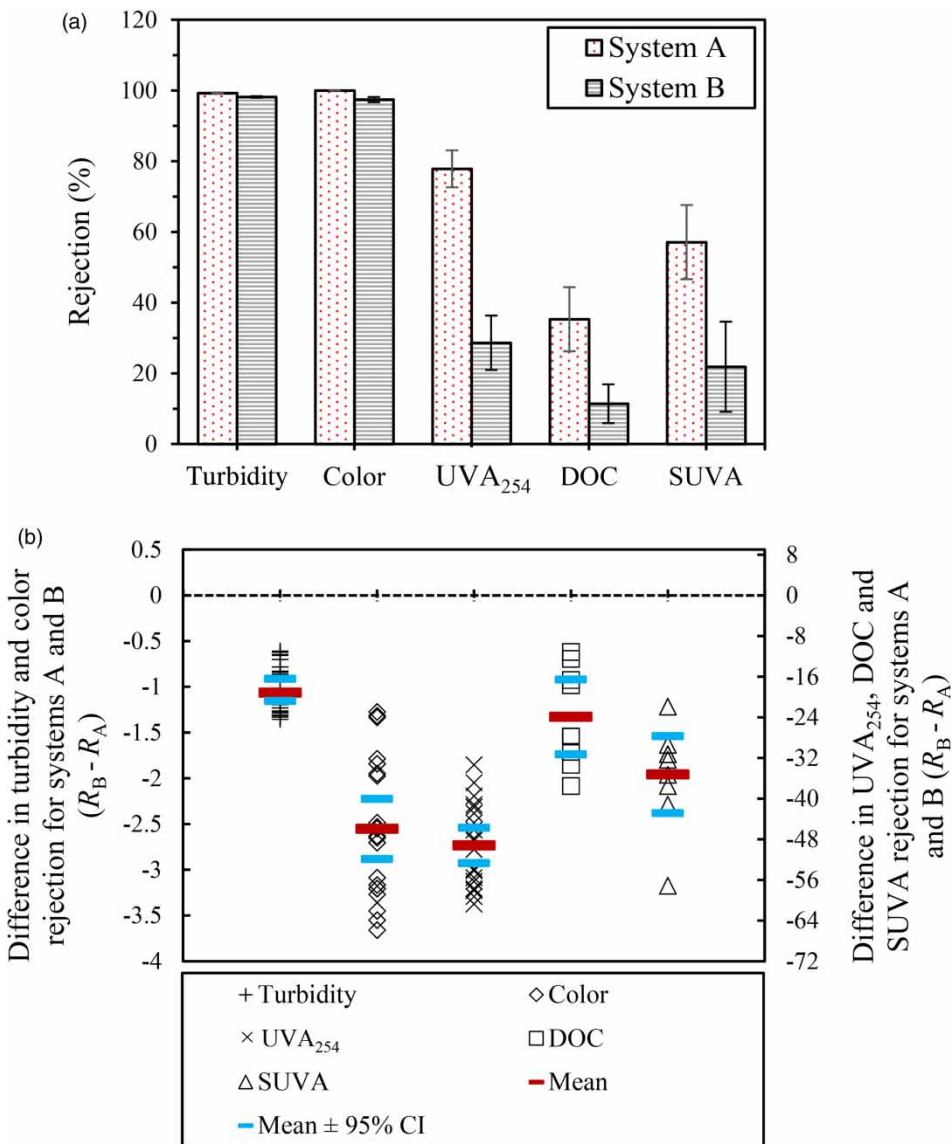

Figure 2 | (a) Average solute rejection and (b) matched-pair analysis for systems A and B. The ordinate in (b) is expressed in terms of system B minus system A values. Turbidity, color, and UVA$_{254}$ analyses are based on 21 pairs of data each while DOC and SUVA are based on nine pairs of data each.

treated water was determined from the SUVA calculations. As shown in Figure 2(a), SUVA removal increased with PACl coagulation. The average percent removals in systems A and B were 57.1% and 21.9%, respectively. A matched-pair analysis was used to statistically evaluate the impact of PACl on the water quality parameters monitored. As shown in Figure 2(b), the line corresponding to $y = 0$ is above the mean $\pm 95\%$ CI range for all the quality parameters assessed, indicating that the differences between system A and B values were statistically different from zero.

Cost analysis and implications for drinking water treatment

In order to compare the costs of the hybrid system with the conventional UF system, a cost analysis was conducted on operating the UF unit with a PACl dose of 1.21 mg-Al·L^{-1} (system A) versus 0 mg-Al·L^{-1} (system B). For a full-scale membrane installation, the net present value (NPV) can be produced from a combination of the capital expenditure (CAPEX) and operating expenditure (OPEX) (Judd 2017). CAPEX includes all equipment, land and installation service costs. OPEX, on the other hand, is mainly determined by the chemical and energy costs, membrane replacement costs, and other items such as labor, water supply, and wastewater discharge costs. The results (Figure 1(a)) suggest that with PACl coagulation, a 21% increase in flux rate could be attained, allowing for a cutback of 27% in the membrane area and a proportionate cutback in CAPEX through membrane costs and reduced footprint. However, PACl dosing increases CAPEX through the installation of a mixing unit, a dosing pump, a chemical storage unit, and a chemical sludge treatment unit. A cost analysis, therefore, proceeds by comparing these two CAPEX elements. Taking the investment cost of the UF membranes to be C_M and the investment cost of a coagulation/flocculation unit to be a logarithmic variant of the Williams Law cost function (Guo *et al.* 2014), then the CAPEX associated with these two elements are given as:

$$\text{CAPEX}_{\text{reduction}} = \frac{1}{C_P}\left(\frac{0.27(C_M + C_L)}{t_M}\right) \tag{5}$$

$$\text{CAPEX}_{\text{increment}} = \frac{1}{C_P}\left(\frac{C_C + C_L}{t_C} + \frac{C_D}{t_D} + \frac{C_S + C_L}{t_S} + \frac{C_{CS} + C_L}{t_{CS}}\right) \tag{6}$$

where C_P is the plant capacity (m^3/d); C_C, C_L, C_D, C_S, and C_{CS} are the cost (USD) of a coagulation unit, land required, dosing pump, chemical storage unit, and chemical sludge treatment unit, respectively; t_M, t_C, t_D t_S, and t_{CS} are the lifespan (d) of the membrane, coagulation unit, dosing pump, chemical storage unit and chemical sludge treatment unit, respectively and

$$\log(C_C) = 0.222 \times (\log(C_P))^{1.516} + 3.071$$

As depicted in Figure 3(a), the principle of economy of scale was found applicable for the impact of PACl dosing on the total investment costs, with a break-even point at 10 m^3/d plant capacity. Thus, for a small community-scale plant with a capacity <10 m^3/d, PACl dosing at 1.21 mg-Al·L^{-1} impacts negatively on the total investment costs. Yet, for larger plants, PACl dosing and higher-flux operation result in an overall reduction in the total investment costs. CAPEX, however, is computed by depreciating investment costs over a period of time and expressed as costs per unit volume of water produced. The results of this conversion are shown in Figure 3(b). It should be noted that UF membranes are packed in modules and so the investment costs increase almost linearly with plant capacity as depicted in Figure 3(c). However, the auxiliary costs associated with coagulation follow the principle of economy of scale (Guo *et al.* 2014), which implies that the costs increase less than linearly with scale as depicted in Figure 3(d). Consequently, as plant capacity increases, CAPEX increments associated with PACl dosing diminish beyond CAPEX reductions resulting from PACl dosing and higher-flux operation, leading to overall savings in CAPEX as shown in Figure 3(b).

As mentioned earlier, the integral costs of a membrane plant consist of both the CAPEX and OPEX. Thus, an outline OPEX analysis on the impact of PACl dosing was also conducted by comparing the reduced cost of membrane replacement vis-à-vis the cost of PACl dosing over the membrane's lifespan (Hatt *et al.* 2011). Taking the membrane costs per m^2 to be C_m and the projected PACl costs per kg to be C_p, then the OPEX associated with these two components are given as:

$$\text{OPEX}_1 = C_m\left(\frac{1}{J_1} - \frac{1}{J_2}\right)\frac{1}{t} \tag{7}$$

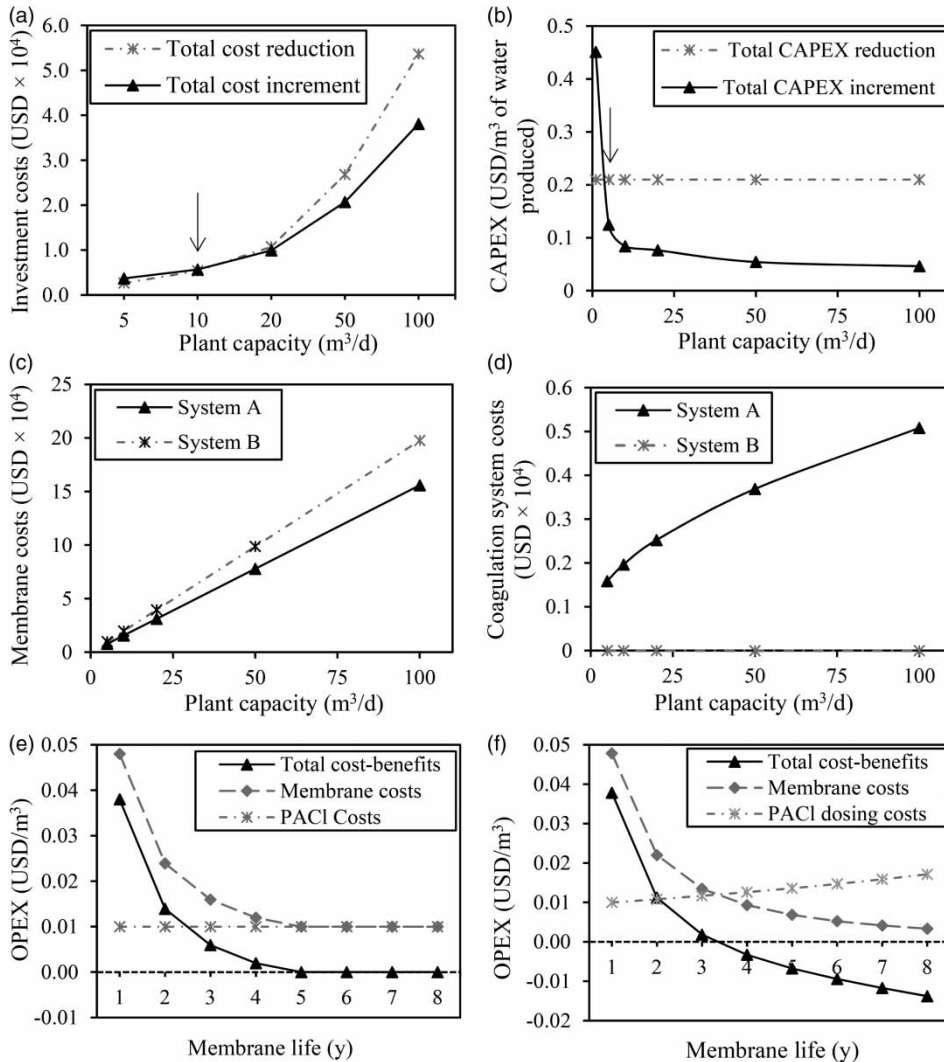**Figure 3** │ Effect of PACl dosing at 1.21 mg-Al·L^{-1} on (a) total investment costs, (b) CAPEX, (c) membrane costs, (d) coagulation system costs, (e) OPEX if PACl and membrane replacement costs remain constant and (f) OPEX if PACl costs increase by 8%, but membrane replacement costs decrease by 8% per annum.

$$OPEX_2 = C_m.d \tag{8}$$

where t is the membrane life (y), J_1 and J_2 are the fluxes at time t with and without PACl, respectively and d is the PACl dose (kg·m^{-3}). As shown in Figure 3(e), PACl dosing at 1.21 mg·Al·L^{-1} provides OPEX benefits in the first 5 y of membrane life based on the current PACl and membrane replacement cost estimates (Table A4, Appendix, available online). Even with a conservative assumption that PACl costs will increase at 8% per annum (p.a.), but the membrane replacement costs will diminish at 8% p.a. due to advances in membrane

technology, PACl dosing provides cost benefits in the initial 3.5 y of membrane life provided the 21% increase in flux rate is sustained (Figure 3(f)). However, considering that the realistic estimate of membrane life is 7 years, PACl dosing will incur a cost penalty of 1 cent/m^3 of water produced (Figure 3(f)). Sensitivity analyses on different PACl and membrane replacement cost assumptions are presented in Figures A4–A6 in the Appendix (available online). Even in a worst-case scenario when PACl costs are projected to increase by 20% p.a. while membrane replacement costs diminish by 20% p.a., PACl dosing still provides cost benefits in the first 2.5 y (Figure A6(e),

Appendix). However, for a membrane life of 7 years, PACl dosing will result in a cost penalty of 3 cents/m^3 of treated water.

It is noteworthy that OPEX analysis based on the assumptions made focuses only on fouling control and does not reflect any added benefits or costs associated with contaminant removal. Considering that PACl dosing at 1.21 mg-Al·L^{-1} provides additional benefits, including enhanced removal of NOM, these additional benefits could offset the presumed OPEX penalty in the worst-case scenario. For instance, higher removal of DOC after coagulation would be expected to reduce chlorine demand and chlorine dose (Xie 2004), which in turn would lower OPEX. However, this justification is probably site-specific and dependent upon the specific characteristics of the source water and the overall treatment goals. For source waters with low aromaticity and no need for enhanced coagulation, increased OPEX due to coagulation cannot be offset by savings in chlorine dosing. Nevertheless, in such scenarios, effective fouling control using low coagulant doses for charge-neutralization, rather than doses for sweep-flocculation, has been shown to provide OPEX benefits (Hatt et al. 2011).

CONCLUSIONS

PACl coagulation ameliorated the permeate flux in the pilot-scale UF unit by significantly suppressing both the total fouling and hydraulically irreversible fouling. Additionally, PACl improved the permeate quality by significantly enhancing turbidity, color, DOC, UVA$_{254}$, and SUVA removal. In comparison with the conventional UF system, the CAPEX of the hybrid coagulation–UF system shows a strong correlation with production capacity. Hence, the hybrid system is more favorable than the conventional UF system at larger capacities. OPEX, on the other hand, appears to be highly correlated to factors such as coagulant and membrane replacement costs, which are also dependent on local variables, including inflation. However, even in the worst-case scenario, OPEX penalties resulting from coagulation could be offset by savings in chlorine dosing. Overall, the results strongly suggest that the hybrid coagulation–UF system is potentially a cost-effective model for decentralized water supply.

REFERENCES

American Public Health Association 2004 Standard Methods for the Examination of Water and Wastewater. APHA/AWWA/WEF, Washington, DC, USA.

Arhin, S. G., Banadda, N., Komakech, A. J., Kabenge, I. & Wanyama, J. 2016 Membrane fouling control in low pressure membranes: a review on pretreatment techniques for fouling abatement. Environmental Engineering Research 21 (2), 109–120.

Arhin, S. G., Banadda, N., Komakech, A. J., Pronk, W. & Marks, S. J. 2018 Optimization of hybrid coagulation–ultrafiltration process for potable water treatment using response surface methodology. Water Science and Technology: Water Supply 18 (3), 862–874.

Bergamasco, R., Konradt-Moraes, L. C., Vieira, M. F., Fagundes-Klen, M. R. & Vieira, A. M. S. 2011 Performance of a coagulation–ultrafiltration hybrid process for water supply treatment. Chemical Engineering Journal 166 (2), 483–489.

Crittenden, J. C., Trussell, R. R., Hand, D. W., Howe, K. J. & Tchobanoglous, G. 2012 MWH's Water Treatment Principles and Design. John Wiley & Sons, Inc., Hoboken, NJ, USA.

Guo, T., Englehardt, J. & Wu, T. 2014 Review of cost versus scale: water and wastewater treatment and reuse processes. Water Science and Technology 69 (2), 223–234.

Hatt, J. W., Germain, E. & Judd, S. J. 2011 Precoagulation-microfiltration for wastewater reuse. Water Research 45 (19), 6471–6478.

Ho, C. C. & Zydney, A. L. 2000 A combined pore blockage and cake filtration model for protein fouling during microfiltration. Journal of Colloid and Interface Science 232 (2), 389–399.

Ho, L., Braun, K., Fabris, R., Hoefel, D., Morran, J., Monis, P. & Drikas, M. 2012 Comparison of drinking water treatment process streams for optimal bacteriological water quality. Water Research 46 (12), 3934–3942.

Howe, K. J. & Clark, M. M. 2006 Effect of coagulation pretreatment on membrane filtration performance. Journal (American Water Works Association) 98 (4), 133–146.

Huang, H., Cho, H.-H., Jacangelo, J. G. & Schwab, K. J. 2012 Mechanisms of membrane fouling control by integrated magnetic ion exchange and coagulation. Environ. Sci. Technol. 46, 10711–10717.

Judd, S. J. 2017 Membrane technology costs and me. *Water Research* **122**, 1–9.

Watkins, K. 2006 *Human Development Report 2006 - Beyond Scarcity: Power, Poverty and the Global Water Crisis*. UNDP Human Development Report, New York, USA.

WHO/UNICEF 2017 *Progress on Drinking Water, Sanitation and Hygiene: 2017 Update and SDG Baselines*. WHO, Geneva, Switzerland, and UNICEF.

Xie, Y. F. 2004 *Disinfection By-Products in Drinking Water: Formation, Analysis, and Control*. Lewis Publishers, CRC Press, Boca Raton, FL, USA.